

Preparation and Investigation of structure, optical , nonlinear optical and thermoelectric properties of Bi₂Se₃ thin film

Ahmed Abdel Moez (✉ aam692003@yahoo.com)

others <https://orcid.org/0000-0002-4755-759X>

H A Elmelgeei

National Research Centre

A I Ali

Helwan University

Research Article

Keywords: Bi₂Se₃ thin film, Optical properties, dielectrical results, nonlinear optical properties, IV characterization and thermoelectric results

Posted Date: March 3rd, 2021

DOI: <https://doi.org/10.21203/rs.3.rs-260695/v1>

License:   This work is licensed under a Creative Commons Attribution 4.0 International License.

[Read Full License](#)

Version of Record: A version of this preprint was published at Materials Technology on July 13th, 2021.

See the published version at <https://doi.org/10.1080/10667857.2021.1954289>.

Preparation and Investigation of structure, optical , nonlinear optical and thermoelectric properties of Bi_2Se_3 thin film

A. Abdel Moez^{*1}, H.A.Elmeleegi² and A.I. Ali³

¹*Solid State Physics Department, Physical Research Division, National Research Centre (NRC), 33 El Bohouth street, Dokki, Giza, P.O.12622, Egypt.*

²*Electronic Microscope Department, Physical Research Division, National Research Centre (NRC), 33 El Bohouth street, Dokki, Giza, P.O.12622, Egypt.*

³*Basic Science Department, Faculty of Technology and Education, Helwan University, Kobry El-Qopa, 11281 Cairo, Egypt*

Abstract

Bi_2Se_3 thin film were prepared using vacuum thermal evaporation technique. the structure and surface topography for this sample were investigated using both of Diffraction Electron Microscope photos (*DEM*) and Transmission Electron Microscope (*TEM*). Bi_2Se_3 thin film had a direct energy gap which was determined by using measured optical parameters such as optical transmittance (T) and optical reflectance (R). The values for both of the oscillating energy (E_o), dispersion energy (E_d) and ratio of the free carrier concentration on the effective mass (N/m^*) were determined optically using the calculated values of refractive index (n). The dielectrical parameters such as dielectric loss (ϵ'') and dielectric tangent loss dielectric loss (ϵ'') were calculated. The density of states (DOS) for both of valence band (N_v) and conduction band (N_c) and also position of Fermi level were determined. The nonlinear optical results such as third-order nonlinear optical susceptibility ($\chi^{(3)}$), nonlinear refractive index (n_2) and nonlinear absorption coefficient (β_c) were determined. The influence of temperature on IV results were studied, finally the dependence of all of Dispersion factor (D), parallel inductance

(L_p) and Seebeck coefficient (S) values on temperature for this film were studied.

Keywords:- Bi_2Se_3 thin film, Optical properties, dielectrical results, nonlinear optical properties, IV characterization and thermoelectric results.

1 Introduction

chalcogenide materials were investigated widely as their optically highly nonlinear, they are sensitivity for absorption of electromagnetic radiation, so they have widely electronic applications[1–4]. Among all these binary chalcogenideis Bi_2Se_3 which is suitable for optical thermoelectric applications[5], solar cell [6], and photosensitive devices, photovoltaic cells, etc. [7-11]. Bi_2Se_3 Thin films have been prepared using various techniques such electro deposition [12] and Successive Ionic Layer Absorption and Reaction (SILAR) [13] methods]. The structure of Bi_2Se_3 thin films were studied[14-20], It was found that, these films had polycrystalline structure with rhombohedral structure of Bi_2Se_3 [17-18], space group ($R\bar{3}m$) (166)[20]. Optical properties of Bi_2Se_3 thin films were studied [21-27], It was found that, the energy gap was 1.51[21], with range 1.4 - 2.25 eV[22], 1.10 eV and decrease with annealing[23], 1.25 eV decrease with substrate temperature[24], 1.22 eV decreased with temperature[25]. the transmitted values increased with annealing[26], The Bi_2Se_3 thin films had a direct transitions[27]. The electrical properties and conductivity mechanism were studied [27-31], It was found that, the electrical conductivity affected strongly with temperature[27], both of electrical resistance [26] and dark resistance[28] decreased with temperature, while the resistivity increase with temperature[29], both of electroconductivity and current densities decrease with temperature[30], electrical conductivity increase with film

thicknesses[31]. Bi₂Se thin films had an excellent thermoelectric properties which were studied widely[32-34]. It was noticed that, the temperature increase electron-hole generation[33]. IV characteristics were studied[35-37]. It was found that, the IV behavior increase with annealing[35]. The nonlinear optical properties of Bi₂Se₃ thin films were investigated[38-40]. It was found that, the surface charge affect on the value of second harmonic generation[39].

In this work we determine the linear and nonlinear optical results, the dielectrical results, IV characterizations and thermo electrical results for Bi₂Se₃ thin films.

2 Experimental Work

Bi₂Se₃ were prepared from Bi and Se pure elements with purity = 99.999%. Since some of elements are reactive at high temperatures with oxygen, synthesis was accomplished in evacuated - silica tubes $\sim 10^{-4}$ Torr and then sealed. The inner walls of silica tubes were coated with pure powder graphite, in order to prevent any reactions between the used elements and silica at elevated temperatures. The sealed silica tubes were heated inside a furnace up to 1150 K and kept at this value for about 10 hours . The homogenized melt was quenched in ice-water, to facilitate rapid quenching the specimens were sealed in tubes with a small diameter (about 2-3mm). Thin film were prepared using vacuum thermal evaporation technique of type Edward- (EDWARDS E 306), the studied films were deposited under vacuum of 10^{-5} torr. The structure of these films was studied using transmission electron microscope of type “JEOL-TEM-1230-Japan made. The optical transmittance and reflectance spectra of these films were measured using double beam spectrophotometer with of type (JASCO corp., v-570) with wavelength range 300-2500 nm.

Current-Voltage properties during illumination with uv-lamp and room light were taken from Virtins Instruments digital- computerized oscilloscope. The electrical measurements was done by Keithley 6517A electrometer.

3 Results and Discussions

3.1 Structure

To confirm the structure of BiSe thin films Diffraction and Electron Microscope photos (*DEM*) with different values of direct magnifications (dirc. magnif.) were obtained as shown in Figs. 1(a,b), with (dirc. magnif. =2500x for (a) and dirc. magnif. =2000x for (b)). The *q*spacing between layers for this sample were determined and illustrated in Table 1, while Transmission Electron Microscope (*TEM*) Images with different values of direct magnifications (dirc. magnif. =2500x for (a) and dirc. magnif. =2000x for (b)) is shown in Figs 2(a,b). From this figure it was noticed that, the grains were distributed all over the film

3.2 Optical results

The measured optical properties such as transmission (*T*), Reflection (*R*) and Absorption (*A*) for this sample is shown in figure 3.

From Fig. 3, it was seen the values of both (*T* and *R*) had a reverse behavior (500-1000 nm), while these values identified from (1000-2500 nm). The absorption coefficient (α) of these investigated films were as [41]

$$\alpha = \frac{1}{d} \ln \left[\frac{(1-R)^2}{T} \right] \quad (1)$$

Where (d) is the film thickness. Fig. 4(a) shows the relation between $(\alpha \cdot hv)^2$ and photon energy (hv) for these films, it was seen that, this film had direct optical energy gap (E_{gdir}) with value 1.98 eV (Table 2).

The Urbach tail for these samples were calculated using the following Equation [42]

$$\alpha = \alpha_o e^{(hv/E_a)} \quad (2)$$

Where E_a is the Urbach constant (tail). In order to determine the Urbach tail. The relation between $\ln(\alpha)$ and (hv) is shown in Fig.4(b). the (E_a) value is in Table 2. The refractive index (n) for this film was calculated as [43]

$$n = \frac{(1 + \sqrt{R})}{(1 - \sqrt{R})} \quad (3)$$

Figure 4(c) shows the dependence of both (n) and extinction coefficient (k) on (λ). From this figure it was seen that, the (n) values decrease with (λ), while (k) values increase (λ), which give indication that, the absorption ability for this sample increase with (λ).

The single oscillator for the Bi_2Se_3 thin film can be expressed by as [44]

$$n^2 - 1 = \frac{E_o - E_d}{E_o^2 - (hv)^2} \quad (4)$$

The values of (E_o) and (E_d) are obtained from the intercept on vertical axis = (E_o/E_d) and the slope = ($E_o E_d$)⁻¹ resulting from Fig. 5(a). The calculated values of (E_o) and (E_d) for these films are shown in Table 2.

The relation between (n^2) and (λ^2) for Bi_2Se_3 thin film in figure 5(b). The values of (N/m^*) for these samples was determined as [45]

$$n^2 - k^2 = \epsilon_L - \left(\frac{eN}{4\pi c^2 \epsilon_o m^*} \right) \lambda^2 \quad (5)$$

Where (ϵ_L) is the lattice dielectric constant, (ϵ_o) is the permittivity of free space, the values of (N/m^*), ϵ_L for these films are shown in Table 2.

The values of (E_o) and (E_d) are listed in Table2, the values of both (M_{-1}) and (M_{-3}) can be derived as [46]:

$$E_o^2 = \frac{M_{-1}}{M_{-3}} \quad (6)$$

$$E_d^2 = \frac{M_{-1}^3}{M_{-3}} \quad (7)$$

The oscillator strength (f) was determined as[47]

$$f = E_o E_d \quad (8)$$

Another important parameter is static refractive index (n_o), which was determined as [48]:

$$n_o = \left[\left(\frac{E_d}{E_o} \right) + 1 \right]^{0.5} \quad (9)$$

The values of both of (ϵ') and (ϵ'') for these samples were determined as [49] :-

$$\epsilon' = (n^2 + k^2) \quad (10)$$

$$\epsilon'' = \left[(n^2 + k^2)^2 - (n^2 - k^2)^2 \right]^{0.5} \quad (11)$$

Figure 6 (a) show the dependence of both (ϵ') and (ϵ'') on ($h\nu$), from this figure it was found that the both (ϵ') and (ϵ'') increase with ($h\nu$).

Real part of optical conductivity (σ_1) and imaginary part of optical conductivity (σ_2) were calculated as [50]

$$\sigma_1 = \frac{(\epsilon'' \cdot c)}{(2\lambda)} \quad (12)$$

$$\sigma_2 = \frac{(1 - \epsilon') \cdot c}{4\lambda} \quad (13)$$

Figure 6(b) show influence of ($h\nu$) on both (σ_1) and (σ_2). From this Fig. it was seen that both (σ_1) and (σ_2) increases with ($h\nu$), while (σ_1) increase

strongly with $(h\nu)$, this gives indication, that this film had a high ability to absorb photons and increase its conductivity.

Linear optical susceptibility $(\chi^{(1)})$ describes the response of the material to photon energy, which determined as [51]:

$$\chi^{(1)} = \frac{(n^2 - 1)}{4\pi} \quad (14)$$

It was found that, $(\chi^{(1)})$ increased with $(h\nu)$ as in in Fig. 6(c), also and the values of $(\chi^{(1)})$ had a maximum values higher than (E_g) this means that this material is a promise material for optical devices.

3.3 Nonlinear optical properties

The third-order nonlinear optical susceptibility $(\chi^{(3)})$ was determined as[52]:

$$\chi^{(3)} = A \left[\frac{E_o \cdot E_d}{4\pi(E_o^2 - (h\nu)^2)} \right]^4 \quad (15)$$

Where $A = 1.7 \times 10^{-10}$ e.s.u [53]. $(\chi^{(3)})$ increase with $h\nu$ as in Fig. 6(c), this could attribud to the variation of free carrier concentration which leads to the increase of electrons mobility, while (n_2) which resulted from nonlinear effects[53] and determined as [54-55]:

$$n_2 = \frac{(12\pi\chi^{(3)})}{n_o} \quad (16)$$

The dependence of (n_2) on (λ) for this thin film is in Fig. 7(a). The values of (n_2) decrease with (λ) . Also (β_c) was determined as [56]:

$$\beta_c = \frac{48 \cdot \pi^3 \cdot \chi^{(3)}}{n^2 \cdot c \cdot \lambda} \quad (17)$$

the values of (β_c) increase with $(h\nu)$ as in Fig. 7(b), as a result high number of excited electron which overcome band gap.

Both of the real and imaginary parts of the third order nonlinear optical susceptibility $(\chi^{(3)})$ were dtermined as follow [57]

$$\text{Re } \chi^{(3)}(esu) = 10^{-4} \left[\frac{\varepsilon_0 c^2 n_0^2 n_2}{\pi} \right] \quad (18)$$

$$\text{Im } \chi^{(3)}(esu) = 10^{-2} \left[\frac{\varepsilon_0 c^2 n_0^2 \lambda \beta}{4\pi^2} \right] \quad (19)$$

The relation between both of $\text{Re } (\chi^{(3)})$ and $\text{Im } (\chi^{(3)})$ are shown in Fig. 7(c), from these figures it is clear that, both of $\text{Re } (\chi^{(3)})$ and $\text{Im } (\chi^{(3)})$ increase with $(h\nu)$, this could be attributed to the increase of electron mobility which gives advanced to high resonance for changing optical properties.

Electrical susceptibility $(\chi_{(e)})$ was determined using the following relation [58]:

$$\chi_{(e)} = \frac{(n^2 - k^2 - \varepsilon_0)}{4\pi} \quad (20)$$

Also relative permittivity ε_r was calculated as [59]:

$$\varepsilon_r = (\chi_e + 1) \quad (21)$$

The dependence of both of $(\chi_{(e)})$ and ε_r on $(h\nu)$ this thin film is shown in Fig. 7(d). It is clear that the values of both of $(\chi_{(e)})$ and (ε_r) with $(h\nu)$; this could be attributed to the increasing of electron mobility with $(h\nu)$.

3.4 Semiconducting and electronic results

The density of states (DOS) are calculated as follow [60]:

$$N_v = 2 \left[\frac{(2\pi m_h^* KT)}{h^2} \right]^{3/2} \quad (22)$$

$$N_c = 2 \left[\frac{(2\pi m_e^* KT)}{h^2} \right]^{3/2} \quad (23)$$

Where (N_v) and (N_c) are the density of states for both valence and conduction bands respectively, effective mass of holes in (Bi_2Se_3) $m_h^* = 0.24m_0$ [61], effective mass of electrons in (Bi_2Se_3) $m_e^* = 0.12m_0$ [62].

The position of Fermi level was determined as [52]:

$$E_f = \left(\frac{KT}{q}\right) \cdot \ln\left(\frac{N_c}{N_v}\right) \quad (24)$$

The values of Fermi level position for this investigated thin film is shown in table 2.

3.5 Electrical and I-V characterization results

The electrical as electrical resistivity and capacitance were studied for this sample. The dependence of both of electrical resistivity ρ and capacitance (C) on temperature Figs. 8 (a,b). From this Fig it was seen that, (ρ) decreased with temperature within temperature range (298 -312 k), this is due to increase of electron mobility with temperature which leads to decrease of resistivity, while within temperature range (328 -348 k) (ρ) increase with temperature due to increase the random motion electrons, which leads to increase the impedance for current passes. On the other hand the capacitance (C) increases with temperature as a result of increase the electron mobility with temperature within temperature range (298-350 k), and decrease within temperature range (353-388 k).

The studied IV characterization is shown in Fig. 9, from this Fig. it was seen that the IV increase linearly with temperature, this due to increase of the electrons mobility's with temperature which leads to increase the passed current. The influence of temperature on measured values of both of (D , L_p and S) with different frequencies are shown in Figs. 10 (a,b,c). From this Fig. it was seen that, (D) increases with both of temperature and frequency as a result of increasing the electron mobility's with temperature, while (L_p) decreases with temperature at low frequencies, while at high frequencies, (L_p) increase with temperature due to increase of electron mobility. Finally (S) increase with temperature as a result of decreasing the electrical resistivity for this film with temperature.

4 Conclusion

The structure and surface topography for this sample were investigated using both of (*DEM*) and (*TEM*) photos, it was found that, the grains were distributed all over the film. Bi_2Se_3 thin film had a direct energy gap with value 1.98 eV. The determined parameters (E_o) and (E_d) had a values of 4.20 and 5.12 eV respectively, while the values of both of (M_{-1} , M_{-3} and f) had a values of 4.68 eV, 2.28 eV and $21.92 (\text{eV})^2$ respectively. The (N/m^*) had a value of $2.3\text{E}+51$. The determined dielectric parameters such as (ϵ^{\prime}) and ($\epsilon^{\prime\prime}$) increase with $h\nu$ as a result of increasing the electron mobility's, the same behavior was obtained for (σ_1, σ_2) with ($h\nu$). The density of states (*DOS*) for both of (N_v) and (N_c) were determined with values of $7.9\text{E}+21$ and $2.2\text{E}+22$ respectively. The values of nonlinear results such as ($\chi^{(3)}$) and (β_c) increase with ($h\nu$) as a result of increase electron mobility and electron response to absorb light beam, also the same results were obtained for both of (χ_e , ϵ_r) with ($h\nu$). The temperature affected strongly on both of electrical resistivity and capacitance for this film. The *IV* results increase with temperature as a result of increase electron mobility's with temperature. The temperature affected strongly on all of (D , L_p and S) which give an advanced to control and change these properties either by change frequency or change temperature.

References

1. A. B. Seddon, Chalcogenide glasses: a review of their preparation, properties and applications. *J. Non-Crystall. Solds.* **184**, 44-50 (1995)
2. J.S. Sanghera, I.D. Aggarwal, Active and passive chalcogenide glass optical fibers for IR applications: a review. *J. Non-Crystall. Solds.* **256–257** 6-16 (1999)
3. V.K. Tikhomirov, Photoinduced effects in undoped and rare-earth doped chalcogenide glasses: review. *J. Non-Crystall. Solds.* **256-257** 328-336 (1999)
4. A. Zakery, S.R. Elliott, Optical properties and applications of chalcogenide glasses: a review. *J. Non-Crystall. Solds.* **330** 1-12 (2003)
5. Y. Kang, Q. Zhang, C. Fan, W. Hu, C. Chen, L.Zhang, F. Yu, Y. Tian, B. Xu, High pressure synthesis and thermoelectric properties of polycrystalline Bi_2Se_3 . *J. Non-Crystall. Solds.* **700(5)**, 223-227 (2017)
6. A. Jagminas, I. Valiunas, G.P. Vernese, R. Juskenas, A. Rutavicius, Alumina template-assisted growth of bismuth selenide nanowire Arrays. *J. Non-Crystall. Solds.* **310**, 428- 433(2008)
7. F. Xiao, C. Hangarter, B. Yoo, Y. Rheem, K. Lee, N.V. Myung, Recent progress in electrodeposition of thermoelectric thin films and nanostructures. *Electrochim.Acta* **53**, 8103-8117(2008)
8. C. Xiao, Z. Li, K. Li, P. Huang and Y. Xie, “Accounts of Chemical Research, Decoupling Interrelated Parameters for Designing High Performance Thermoelectric Materials, ” *Accounts of Chemical Research* **47**, 1287-1295 (2014).

9. J. Ko, J. Kim, S. Choi, Y. Lim, W. Seo, K. Lee, Nanograined thermoelectric $\text{Bi}_2\text{Te}_{2.7}\text{Se}_{0.3}$ with ultralow phonon transport prepared from chemically exfoliated nanoplatelets. *J. Mater. Chem. A* **1**, 12791-12796 (2013).
10. S. Borisova, J. Krumrain, M. Luysberg, G. Mussler, D. Gruitzmacher, Crystal Growth & Design, Mode of Growth of Ultrathin Topological Insulator Bi_2Te_3 Films on Si (111) Substrates. *Cryst. Grow. Desgn.* **12**, 6098-6103 (2012).
11. H. Tang, D. Liang, L.J.R. Qiu X.P.A. Gao, Two-Dimensional Transport-Induced Linear Magneto-Resistance in Topological Insulator Bi_2Se_3 Nanoribbons. *ACS nano* **59**, 7510-7516 (2011)
12. A.P. Torane, C.D. Lokhande, P.S. Patil, C.H. Bhosale, Preparation and characterization of electrodeposited Bi_2Se_3 thin Films. *Mater. Chem. Phys.* **55**, 51-54(1998)
13. B.R. Sankapal, R.S. Mane, C.D. Lokhande, Preparation and characterization of Bi_2Se_3 thin films deposited by successive ionic layer adsorption and reaction (SILAR) method. *Mater. Chem. Phys.* **63(3)**, 230-234 (2000)
14. N.D. Desai, V.B. Ghanwat, KV. Khot, S.S. Mali, C.K. Hong, P.N. Bhosale, Effect of substrate on the nanostructured Bi_2Se_3 thin films for solar cell applications, *J. Mater.Sci.: Mater. Electron.* **27**, 2385-2393 (2016)
15. R. Harpeness, A. Gedanken, Microwave-assisted synthesis of nanosized Bi_2Se_3 . *Nw. J. Chem.* **27**, 1191-1193(2003)
16. S. D. Kharade, N.B. Pawar, V. B. Ghanwat, S. S. Mali, W. R. Bae, P.S. Patil, C.K. Hong, J-H. Kim, P.N. Bhosale, Room temperature deposition of nanostructured Bi_2Se_3 thin films for photoelectrochemical application: effect of chelating agents. *Nw. J. Chem.* **37**, 2821-2828 (2013)

17. B. Irfan, R. Chatterje, Characterization and synthesis of Bi_2Se_3 topological insulator thin film using thermal evaporation. *Advan. Mater. Lett.* **7(10)**, 100-150 (2016).
18. P. Plachinda, M. Hopkins, S. Rouvimov, R. Solanki, Topological Insulator Bi_2Se_3 Films on Silicon Substrates. *J. Electr. Mater.* **49**, 2191-2196 (2020).
19. S.K. Jerng, K. Joo, Y. Kim, S.M. Yoon, J.H. Lee, M. Kim, J.S. Kim, E. Yoon, S. H. Chuna, Y.S. Kim, Ordered growth of topological insulator Bi_2Se_3 thin films on dielectric amorphous SiO_2 MBE. *Nanoscale* **5**, 10618-10622 (2013).
20. C. Han, J. Yang, C. Yan, Y. Li, F. Liu, L. Jiang, J. Ye, Y. Liu, The electrochemical self-assembly of hierarchical dendritic Bi_2Se_3 Nanostructures. *CrystEngComm.* **16**, 2823-2834 (2014).
21. A.M. Adam, E. Lilov, E. M.M. Ibrahim, P. Petkov, L.V. Panina M.A. Darwish, Correlation of structural and optical properties in as-prepared and annealed Bi_2Se_3 thin films. *J. Mater. Process. Technol.* **264**, 76-83 (2019)
22. V.T. Patil, Y.R. Toda, D.N. Gujarathi, Structural, Transport and Optical Properties of Nanostructured Vacuum Evaporated Bi_2Se_3 Thin Films. *Intern. J. Scientif. Engineer. Resear.* **5**, 1220-1227 (2014)
23. S. Meyvela, P. Sathyab, M. Parthibavarmana, Annealing Effect on Structural, Optical and Electrical Properties of Bismuth Selenide Thin Films Using Chemical Bath Deposition Method. *Elixir Intern. J.* **101**, 43922-43926 (2016).
24. C.M. Muiva, C. Moditswe, T.S. Sathiaraj, Chemical Synthesis and Properties of Novel Bi_2Se_3 Nanostructures and Microplatelets. *Intern. Schol. Resear. Notic.* **2012**, 6 pages (2012).
25. A.G. Kannan, T.E. Manjulavalli, Structural, optical and electrical

- properties of Bi_2Se_3 thin films prepared by spray pyrolysis technique. Intern. J. ChemTech Resear. **8**, 599-606 (2015).
26. B. Pejova, I. Grozdanov, Chemical deposition and characterization of glassy bismuth(III) selenide thin films. Thn. Sold. Flms. **408**, 6-10 (2002).
 27. S. Augustine, J. K. Kang, E. Mathai, S. Ampili, Structural, electrical and optical properties of Bi_2Se_3 and $\text{Bi}_2\text{Se}_{(3-x)}\text{Te}_x$ thin films. Mater. Resear.Bull. **40**, 1314-1325 (2005).
 28. B. Pejova , I. Grozdanov, A. Tanuevski, Optical and thermal band gap energy of chemically deposited bismuth(III) selenide thin films. Mater.Chemi. Phys.**83**, 245-249 (2004).
 29. Y.C. Lin, Y.S. Chen, C.C. Lee, J.K. Wu, H.Y. Lee, C.T. Liang, Y.H. Chang , “A study on the epitaxial Bi_2Se_3 thin film grown by vapor phase epitaxy. AIP Advan. **6**, 065218-065219 (2016)
 30. V.V. Chistyakov, A.N. Domozhirova, J.C.A. Huang, V.V. Marchenkov, Thickness dependence of conductivity in Bi_2Se_3 topological insulator. J.Phy. Confer. Ser.**1389**, 012051-012055(2019)
 31. S.I. Menshikova, E.I. Rogacheva, A. Yu. Sipatov, A.G. Fedorov, Dependence of electrical conductivity on Bi_2Se_3 thin film thickness. Function. Mater. **24(4)**, 555-558 (2017)
 32. M. Guo, Z. Wang, Y. Xu ,H. Huang, Y. Zang, C. Liu, W. Duan, Z. Gan, S. C. Zhang, K. He, X. Ma, Q. Xue, Y. Wang, Tuning thermoelectricity in a Bi_2Se_3 topological insulator via varied Film thickness. Nw. J. Phys. **18**, 015008-15014 (2016).
 33. D. Kim, P. Syers, N.P. Butch, J. Paglione, M.S. Fuhrer, Ambipolar Surface State Thermoelectric Power of Topological Insulator Bi_2Se_3 . Nano Lett. **14**, 1701-1706 (2014).
 34. P.H. Le, C.N. Liao, C.W. Luo, J.Y. Lin, J. Leu, Thermoelectric

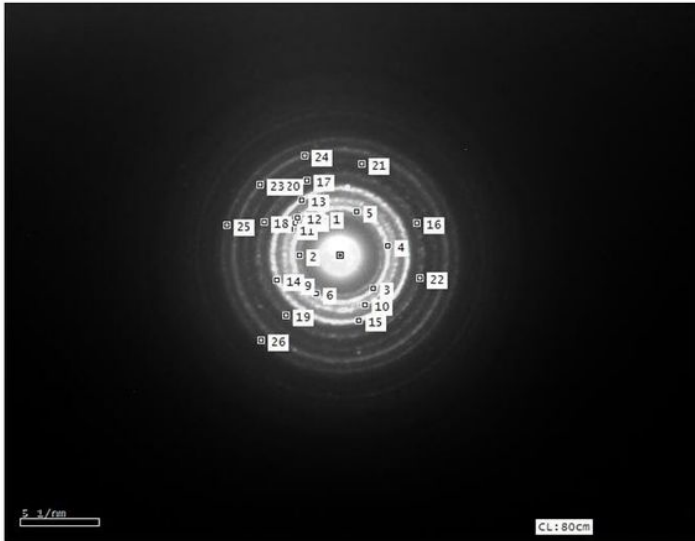
- properties of bismuth-selenide films with controlled morphology and texture grown using pulsed laser deposition. *Appl. Surf. Sci.* **285**, 657-663 (2013).
35. B. R. Sankapal, H. M. Pathn and C. D Lokhande, Photoelectrochemical (PEC) studies on chemically deposited Bi_2Se_3 thin films. *Ind. Jo. Pre. Appl. Phys.* **40**, 331-336 (2002)
 36. Q. Zhang, Two-Dimensional Tunnel Transistors Based on Bi_2Se_3 Thin Film. *IEEE Electr.Devc. Lett.* **35(1)**, 129-131 (2014).
 37. L. Xiao, Q. Liu, M. Zhang, L. Liu, Photoelectric properties of Bi_2Se_3 films grown by thermal evaporation method. *Mater. Resear. Exprss.* **7**, 016429-016435 (2020).
 38. Y. Tan, Z. Guo, Z. Shang, F. Liu, R. Böttger, S. Zhou, J. Shao, X. Yu, H. Zhang, F. Chen, Tailoring nonlinear optical properties of Bi_2Se_3 through ion irradiation. *Scientif. Reprt.* **6**, 21799-21805 (2016)
 39. S. Lu, C. Zhao, Y. Zou, S. Chen, Y Chen, Y. Li, H. Zhang, S. Wen, D. Tang, Third order nonlinear optical property of Bi_2Se_3 . *Optics. Exprss.* **21**, 2072-2082 (2013)
 40. D. Hsieh, J.W. McIver, D.H. Torchinsky, D.R. Gardner, Y.S. Lee and N. Gedik, Nonlinear Optical Probe of Tunable Surface Electrons on a Topological Insulator. *Phys. Rev. Lett.* **106**, 057401-057404 (2011).
 41. M. Fadel, S.A. Fayek, M.O. Abou-Helal, M.M. Ibrahim, A.M. Shakra, Structural and optical properties of SeGe and SeGeX ($X = \text{In, Sb and Bi}$) amorphous films. *J.Allys. Compuds.* **485**, 604-609 (2009).

42. F. Urbach, The Long-Wavelength Edge of Photographic Sensitivity and of the Electronic Absorption of Solids. *Phys. Rev.* **92**, 1324-1324 (1953)
43. *Optical Process in semiconductors*, edited by J.I. Pankove, Dover Publications, Inc., New York, (1971)
44. J. Torris, J.I. Cisneros, G. Gordillo, F. Alvarez, A simple method to determine the optical constants and thicknesses of $Zn_xCd_{1-x}S$ thin films. *Thin. Solid. Flms.* **289**, 238-241 (1996)
45. A.I. Ali, J.Y. Son, A.H. Ammar, A. Abdel Moez, Y.S. Kim, Optical and dielectric results of $Y_{0.225}Sr_{0.775}CoO_{3\pm\delta}$ thin films studied by spectroscopic ellipsometry technique. *Reslt. Phys.* **3**, 167-172 (2013)
46. A.M. Farid, I.K. El-Zawawi, A.H. Ammara, Compositional effects on the optical properties of $Ge_xSb_{40-x}Se_{60}$ thin films, ” *Vacuum* **86** 1255-1261(2012).
47. S.H. Wemple, M. DiDomenico, Jr., Optical Dispersion and the Structure of Solids, *Phys. Rev. Lett.* **23**, 1156-1156 (1969)
48. K. Anshu, A.Sharma, Study of Se based quaternary $SePb(Bi,Te)$ chalcogenide thin films for their linear and nonlinear optical properties *Optk.* **127** 48-54(2016)
49. A.B. Djuriscic, E. H.Li, Modeling the optical properties of sapphire ($\alpha-Al_2O_3$). *Optics. Commun.* **157**, 72-76 (1998).
50. A.H. Ammar, A.M. Frid, M.A.M. Sayam, Heat treatment effect on the structural and optical properties of $AgInSe_2$ thin films. *Vacum.* **66**, 27-38 (2002).
51. S.E. Fritz and T.W. Kelley, C.D. Frisbie, Effect of Dielectric Roughness on Performance of Pentacene TFTs and Restoration of Performance with a Polymeric Smoothing Layer. *J. Phys. Chem. B* **109**, 10574-10577 (2005).

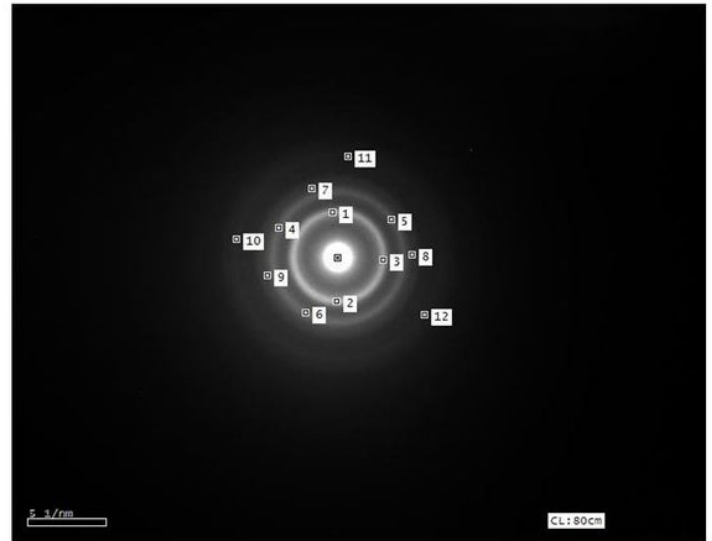
52. A.A. Ziabari, F.E. Ghodsi, Optoelectronic studies of sol–gel derived nanostructured CdO–ZnO composite films. *J. Allys. Compu.* **509**, 8748-8755 (2011).
53. R.H. Stolen, A. Ashkin, Optical Kerr effect in glass waveguide. *Appl. Phys.Lett.* **22**, 294 (1973).
54. H. Tichá, L. Tichy, Semiempirical relation between non-linear susceptibility (refractive index), linear refractive index and optical gap and its application to amorphous chalcogenides. *J. Optoelectron. Advan. Mater.* **4(2)**, 381-386 (2002).
55. P. Zhou, G. You, J. Li, S. Wang, S. Qian, L. Chen, Annealing effect of linear and nonlinear optical properties of Ag: Bi₂O₃ nanocomposite films. *Optics. Exprss.* **13**, 1508-1514 (2005).
56. B. Derkowskaa, B. Sahraouia, X.N. Phua, W. Bala, Nonlinear optical properties in ZnSe crystals. *Proceed. of SPIE*, **4412**, 373-341 (2001)
57. R.N. Shaikh , Mohd.Anis , M.D. Shirsat, S.S. Hussaini, Investigation on the Linear and Nonlinear Optical Properties of L-Lysine Doped Ammonium Dihydrogen Phosphate Crystal for NLO Applications. *IOSR J. Appl. Phys.***6(1)**, 42-46 (2014)
58. V. Gupta, A.I. Mansingh, Influence of post deposition annealing on the structural and optical properties of sputtered zinc oxide film. *J. Appl. Phys.* **80**,1063 (1996)
59. S.E. Braslavsky. Glossary of terms used in photochemistry. *Pur. Appl.Chem.* **79**, 293-465 (2007)
60. S.M. Sze, *Physics of Semiconductor Devices* (Wiley-Interscience, New York, 1969).
61. G. Martinez, B.A. Piot, M. Hakl, M. Potemski, Y.S. Hor, A. Materna, S.G. Strzelecka, A. Hruban, O. Caha, J. Novák, A. Dubroka, Č. Drašar, M. Orlita, “Determination of the energy

- band gap of Bi_2Se_3 . *Scientif. Reprt.* **7**, 6891-6895(2017).
62. A.B. Sushkov, G.S. Jenkins, D.C. Schmadel, N.P. Butch, J. Paglione, H.D. Drew, Far-infrared cyclotron resonance and Faraday effect in Bi_2Se_3 . *Phys. Rev. B* **82**, 125110 (2010).

Figures



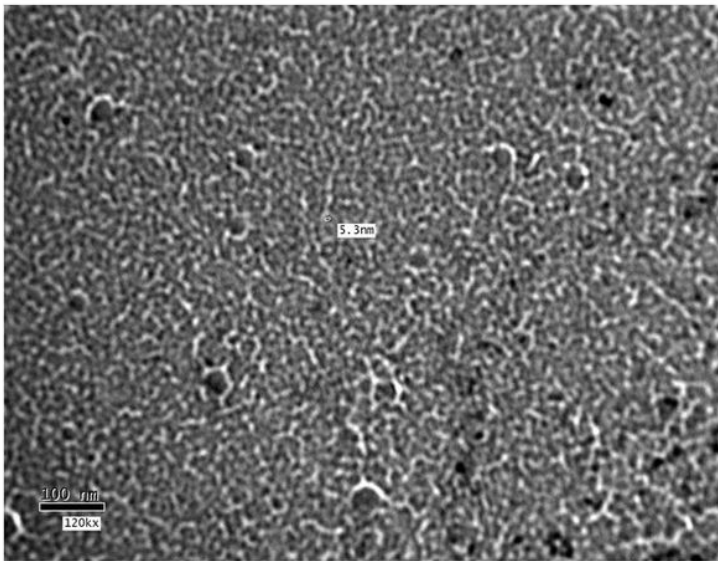
(a)



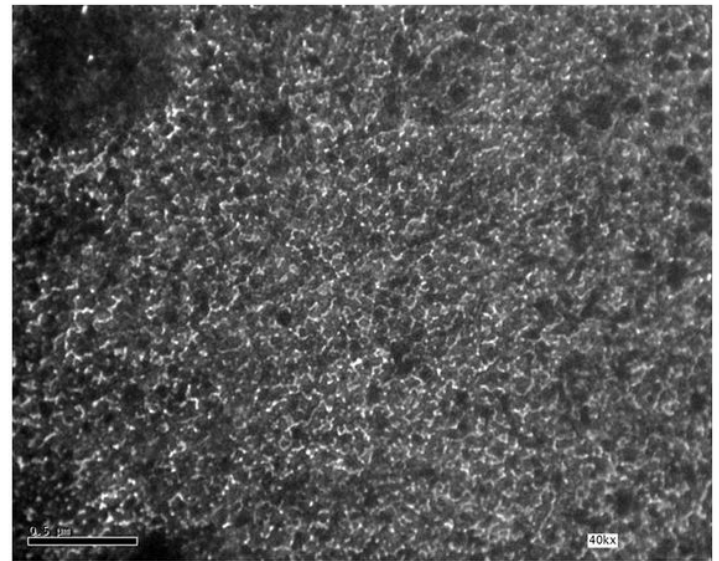
(b)

Figure 1

DEM Images a with dir. magnif. =2500x and b dir. magnif. =2000x for for Bi₂Se₃ thin films.



(a)



(b)

Figure 2

TEM Images with a dir. magnif. =2500x and b dir. magnif. =2000x for Bi₂Se₃ thin films.

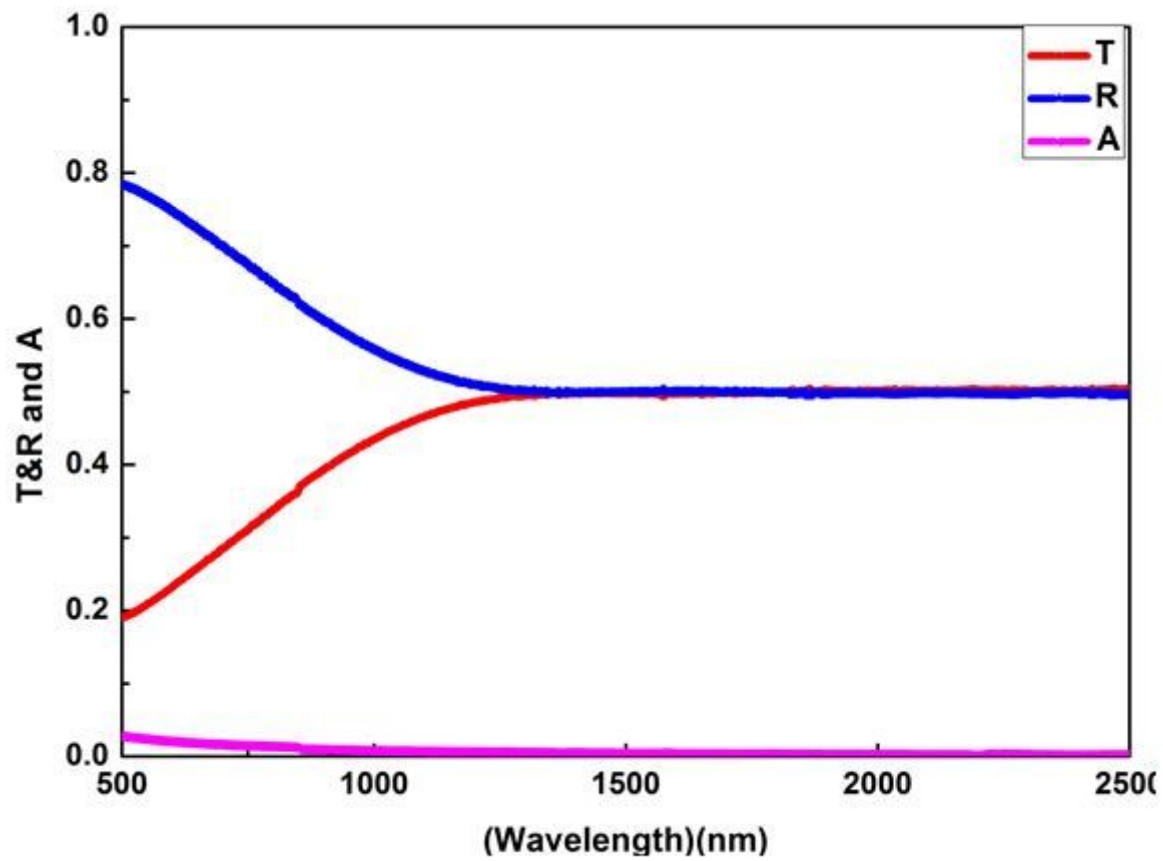


Figure 3

The optical measured parameters such as, Transmittance, Reflectance and Absorbance for Bi₂Se₃ thin film.

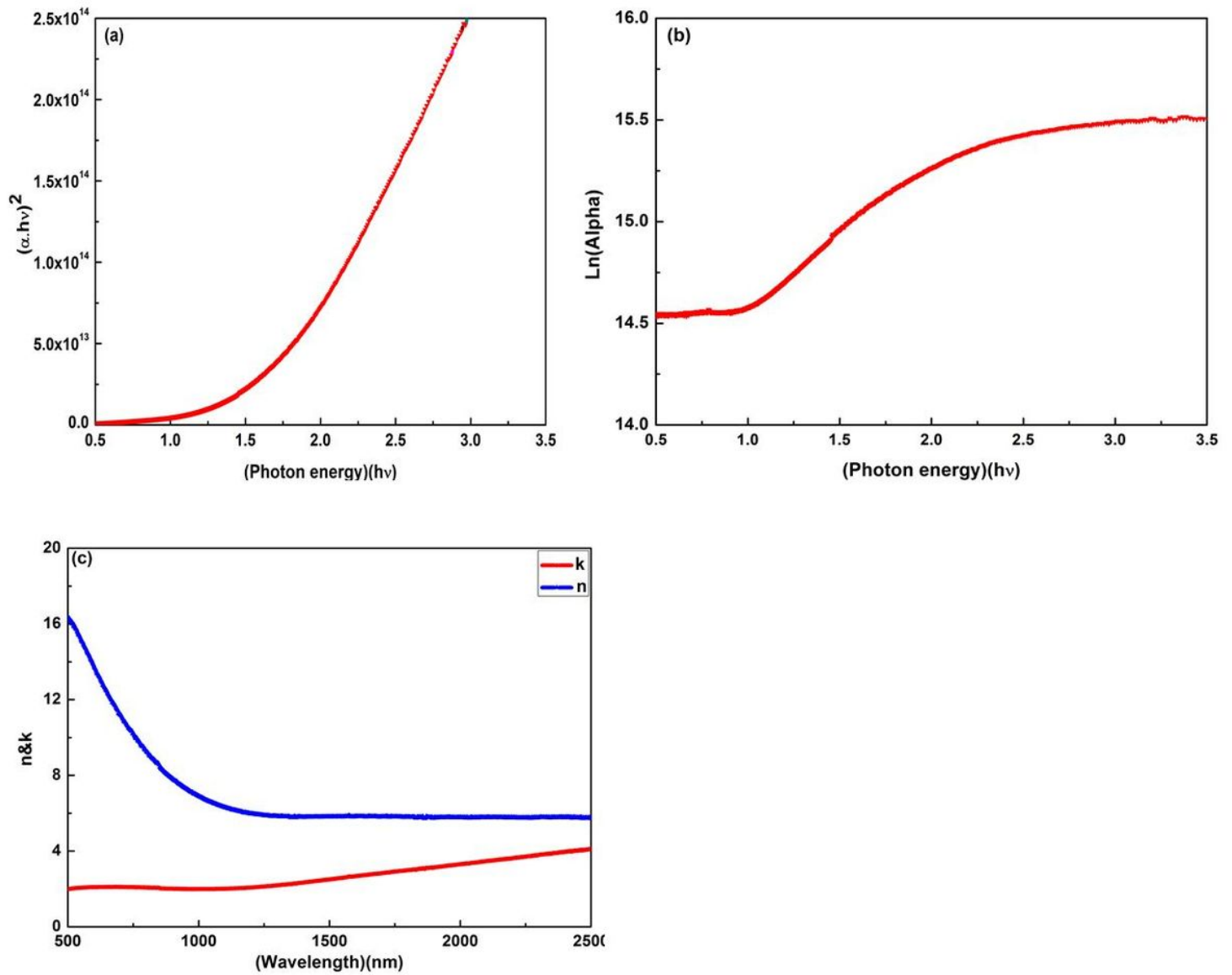


Figure 4

a relation between $h\nu$ and $(\alpha \cdot h\nu)^2$, b the dependence of $\ln \alpha$ on $h\nu$ and c the relation between both of (n, k) and λ for Bi₂Se₃ thin film.

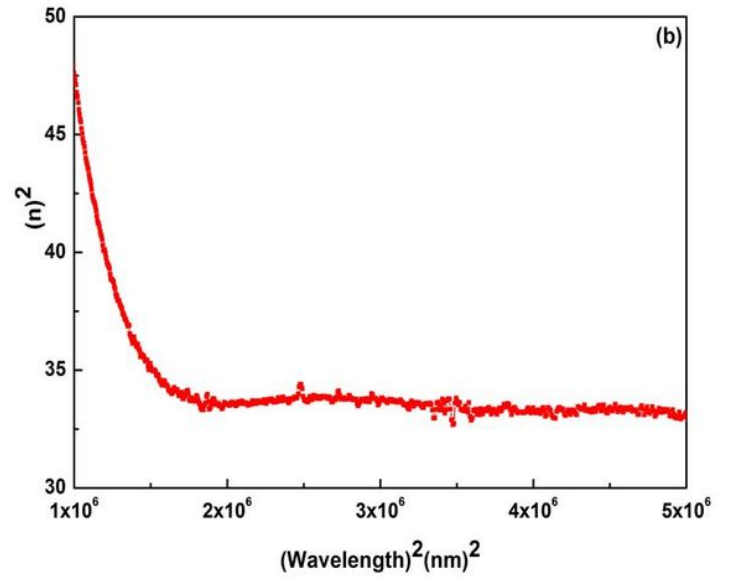
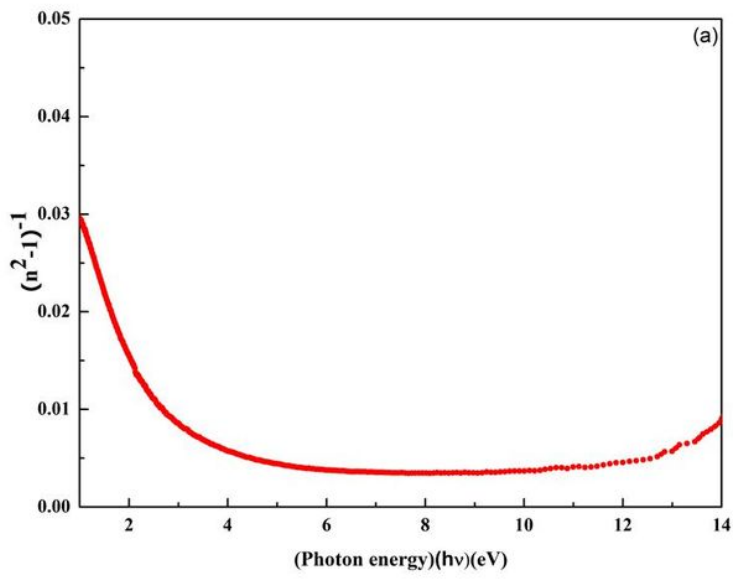


Figure 5

a The dependence of $(n^2-1)^{-1}$ on $(h\nu)^2$ and b the dependence of n^2 on λ^2 for Bi_2Se_3 thin film.

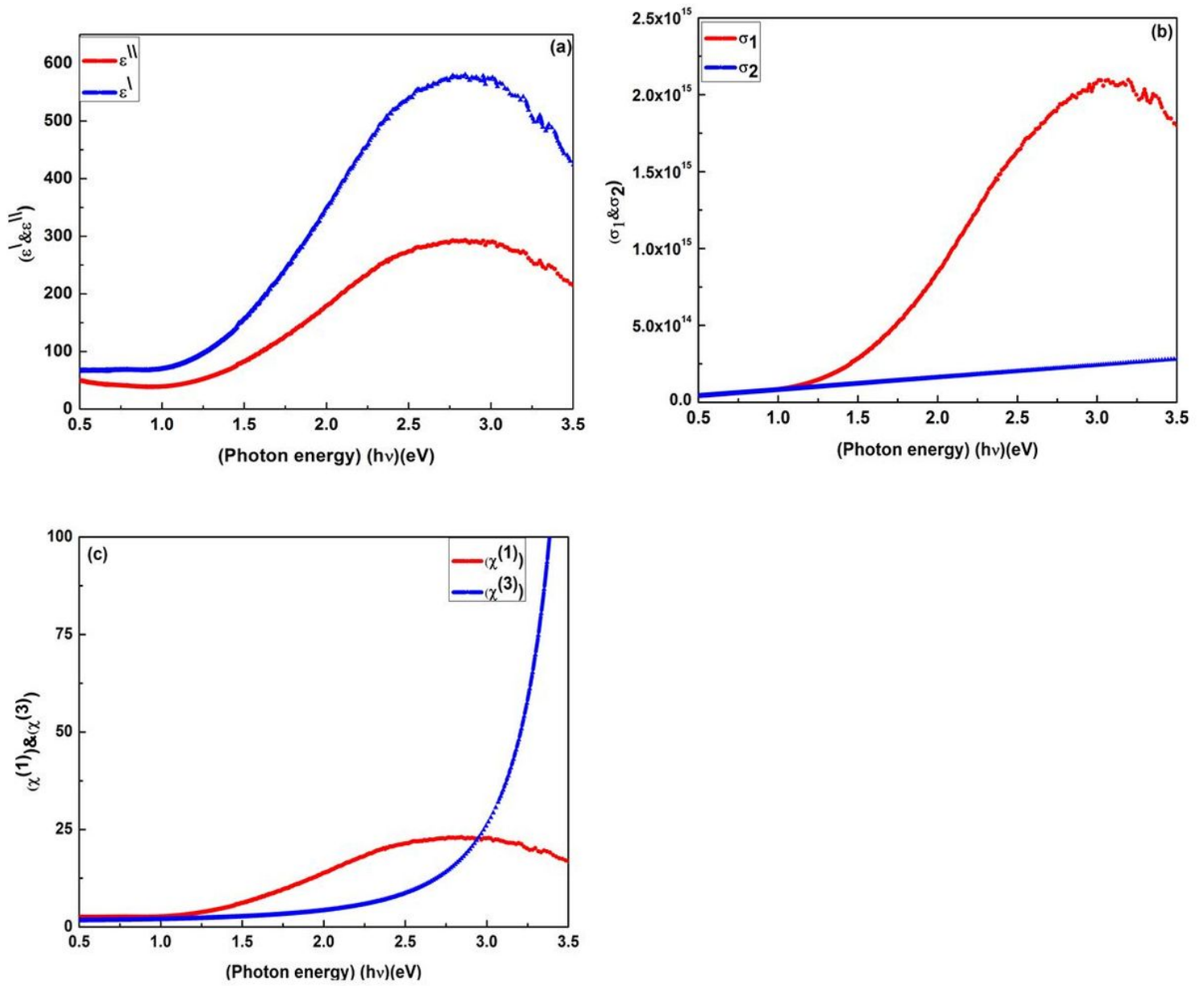


Figure 6

a The influence of $h\nu$ on (ϵ', ϵ'') , b the dependence of both of on (σ_1, σ_2) on $h\nu$ and c the The influence of $h\nu$ on $\chi^{(1)}, \chi^{(3)}$ for Bi₂Se₃ thin film.

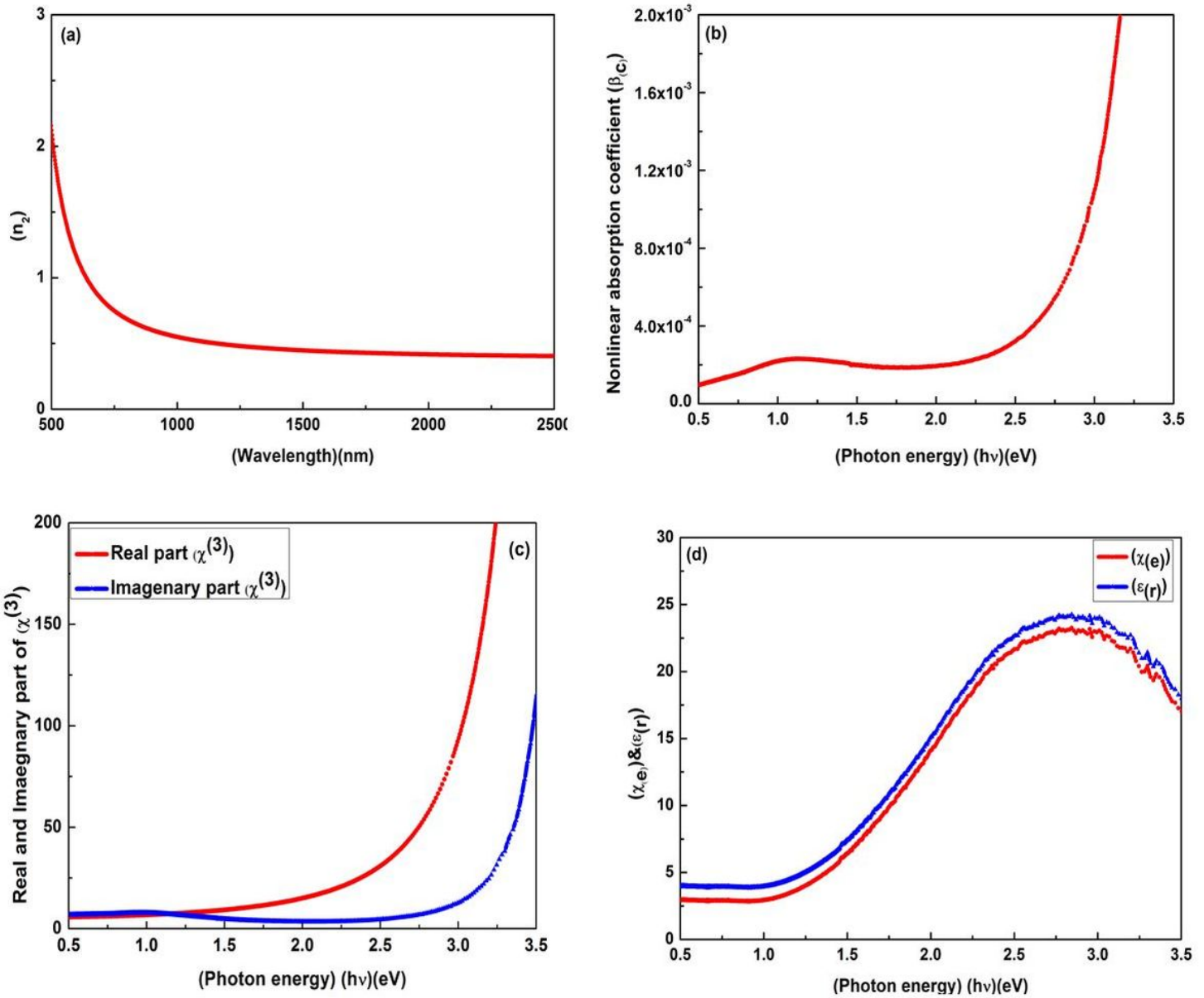


Figure 7

a the dependence of n_2 on λ , b the influence of $h\nu$ on β_c , c the dependence of both of real $\chi^{(3)}$, $\text{Im} \chi^{(3)}$ on $h\nu$ and d the dependence of both of (χ_e, ϵ_r) on $h\nu$ for Bi₂Se₃ thin film.

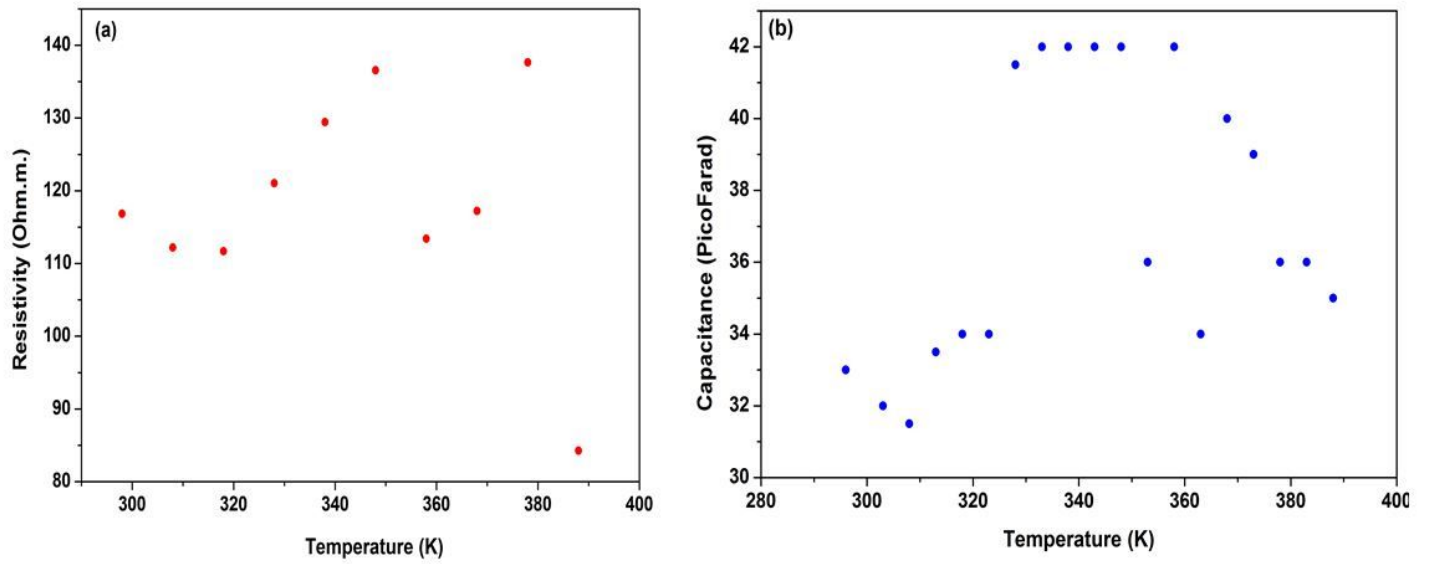


Figure 8

The influence of temperature on both of resistivity a and capacitance b for Bi₂Se₃ thin film.

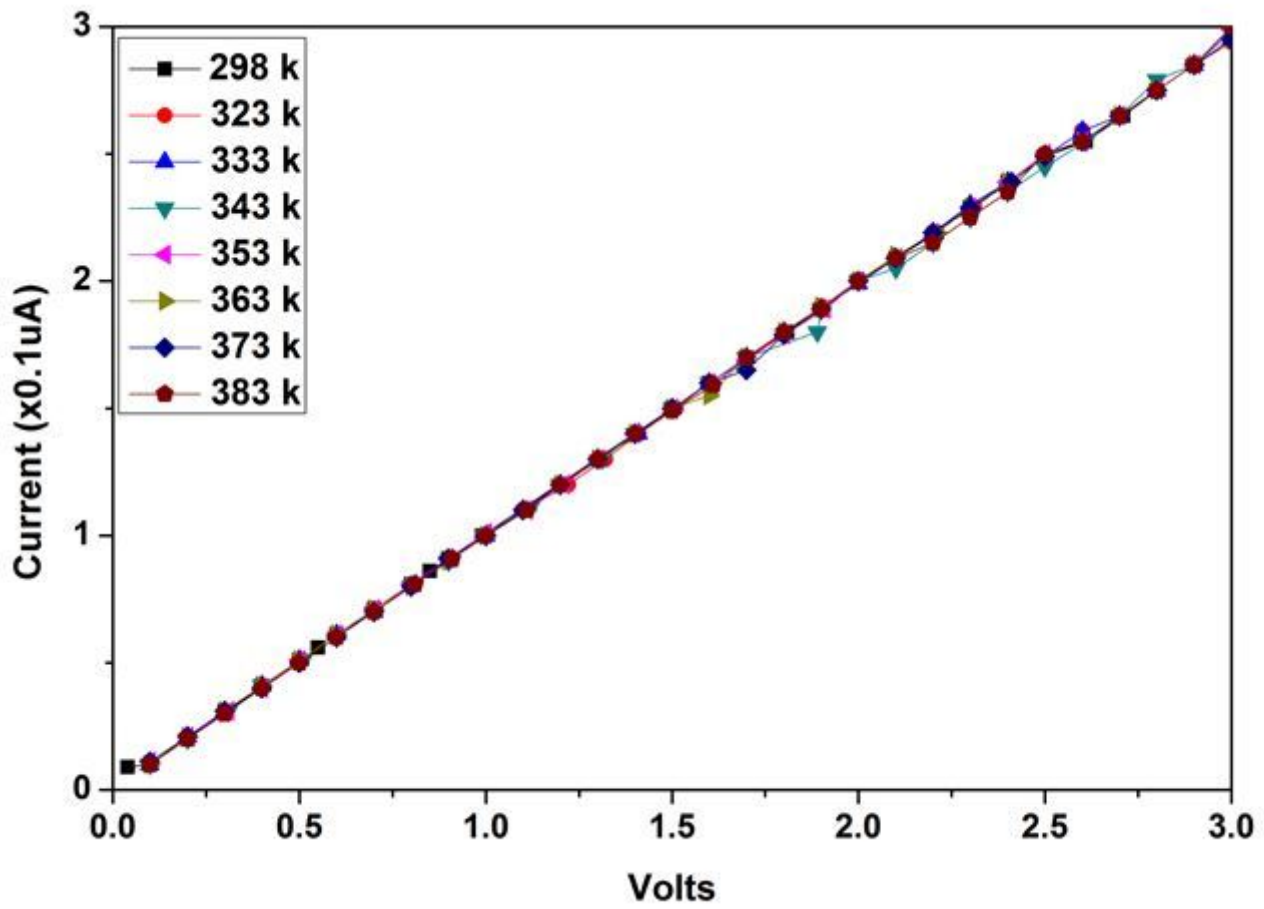


Figure 9

The influence of temperature on IV characterization for Bi₂Se₃ thin film.

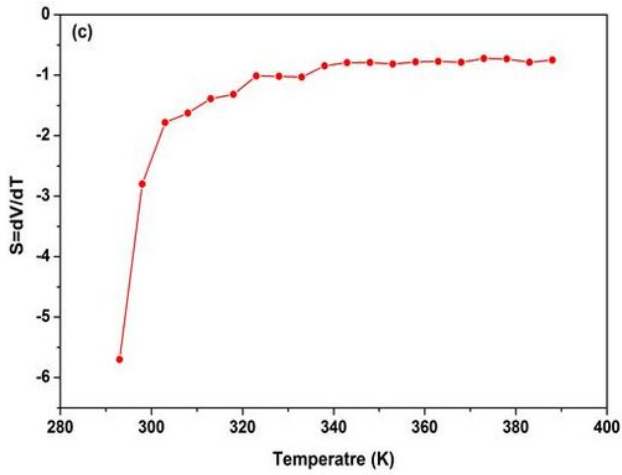
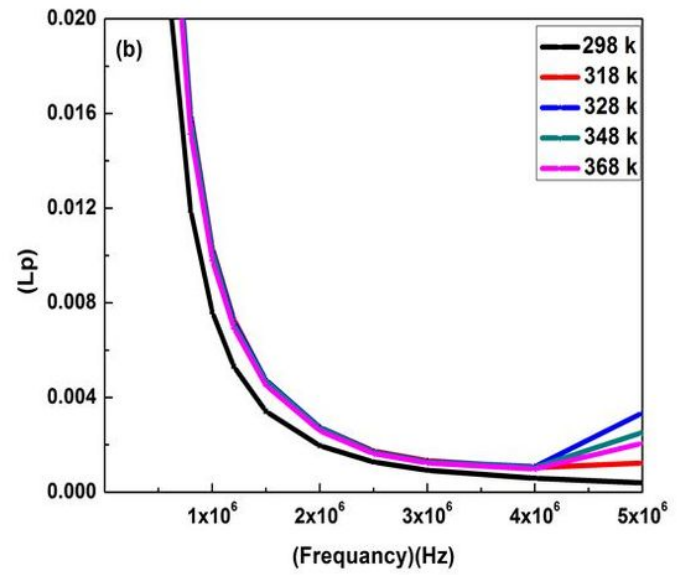
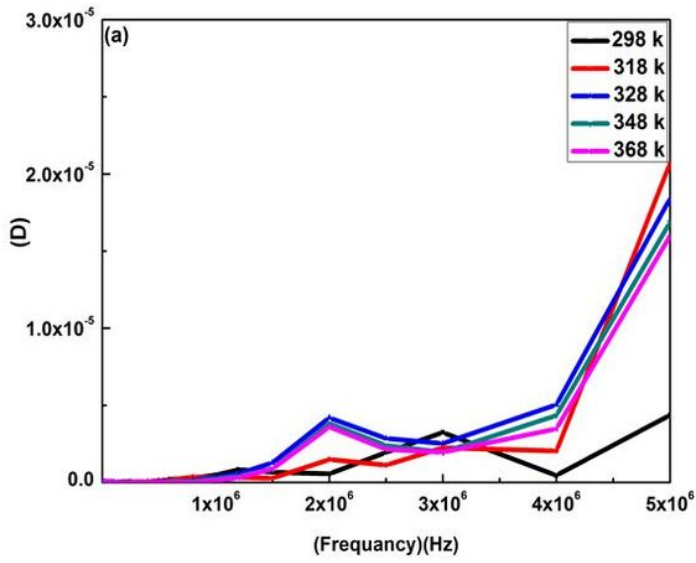


Figure 10

a The relation between frequency and D , b frequency and L_p at different temperature, c relation between S and temperature for Bi_2Se_3 thin film.